

# Numerical aperture dependence of damage and supercontinuum generation from femtosecond laser pulses in bulk fused silica

Jonathan B. Ashcom,\* Rafael R. Gattass, Chris B. Schaffer,<sup>†</sup> and Eric Mazur

*Department of Physics and Division of Engineering and Applied Sciences, Harvard University, 9 Oxford Street, Cambridge, Massachusetts 02138*

Received January 13, 2006; revised July 18, 2006; accepted July 23, 2006; posted July 26, 2006 (Doc. ID 66335)

Competing nonlinear optical effects are involved in the interaction of femtosecond laser pulses with transparent dielectrics: supercontinuum generation and multiphoton-induced bulk damage. We measured the threshold energy for supercontinuum generation and bulk damage in fused silica using numerical apertures (NAs) ranging from 0.01 to 0.65. The threshold for supercontinuum generation exhibits a minimum near 0.05 NA and increases quickly above 0.1 NA. For NAs greater than 0.25, we observe no supercontinuum generation. The extent of the blue broadening of the supercontinuum spectrum decreases significantly as the NA is increased from 0.01 to 0.08, showing that weak focusing is important for generating the broadest supercontinuum spectrum. Using a light-scattering technique to detect the onset of bulk damage, we confirmed bulk damage at all NAs studied. At a high NA, the damage threshold is well below the critical power for self-focusing. © 2006 Optical Society of America

OCIS codes: 320.2250, 260.5950, 140.3440, 160.6030.

## 1. INTRODUCTION

When femtosecond pulses are strongly focused into a transparent material, permanent damage can be produced in the bulk of the material via nonlinear absorption.<sup>1–3</sup> Although weakly focused femtosecond pulses can also produce bulk damage,<sup>4,5</sup> significantly more energy is required than under strong-focusing conditions and such pulses tend to generate a considerable amount of supercontinuum light.<sup>6</sup> The pulse's spectrum broadens considerably as it propagates, resulting in the formation of a broad flat pedestal on the blue side of the spectrum (blue broadening).<sup>6,7</sup> The fact that otherwise identical laser pulses produce damage when strongly focused and generate a supercontinuum when weakly focused shows that the numerical aperture (NA) is a critical parameter that governs how femtosecond laser pulses interact with and propagate in transparent materials. In this paper we study how the focusing conditions affect bulk damage and supercontinuum generation by femtosecond laser pulses in fused silica.

Laser-induced breakdown and supercontinuum generation have been studied extensively.<sup>6–9</sup> The role of focusing conditions in the breakdown and supercontinuum generation in CO<sub>2</sub> gas and in water has been investigated with picosecond<sup>10,11</sup> and femtosecond pulses.<sup>12</sup> The effect of the NA on femtosecond pulse propagation and supercontinuum generation has also been investigated in solids using numerical simulations<sup>13,14</sup> and experimentally in fused silica.<sup>9</sup> The experimental work in fused silica, however, was limited to NAs ranging from 0.03 to 0.29 and identified the detection of radiation at 400 nm as the threshold for supercontinuum, as opposed to looking for the onset of blue broadening.

Here we report the results of a systematic study of the

energy threshold for bulk damage and supercontinuum generation using femtosecond pulses in fused silica as a function of the NA of the external focusing optics. While femtosecond pulse-induced damage is an intensity-dependent effect, self-focusing makes the unambiguous determination of the focused spot size within the bulk challenging, and hence we use the pulse energy as the fundamental quantity in this study, as it is the quantity over which the experimenter has direct control. Our results indicate that the interaction of femtosecond laser pulses with transparent materials falls into three regimes, depending on the NA. We find that bulk damage can be produced at all NAs investigated ( $0.1 < \text{NA} < 0.65$ ), but that supercontinuum generation does not occur at 0.25 NA or higher (the “high-NA regime”). In the range from 0.05 to 0.15 NA (the “medium-NA regime”), we observe the supercontinuum generation, but multiple shots show the accumulation of bulk damage, causing the supercontinuum to disappear. Finally, below 0.05 NA (the “low-NA regime”), it is possible to damage the bulk, but only at energies significantly above the threshold for the supercontinuum generation. The morphology of the damage is found to be different for high and low NA. For damage induced at low NAs, we observe multiple refocusing of the femtosecond laser pulse. We also show that the extent of the blue broadening in the supercontinuum diminishes with an increasing NA.

## 2. EXPERIMENTAL SETUP

The experiments were carried out using a multipass-amplified Ti:sapphire laser operating at 1 kHz with a center wavelength of 800 nm, a 40 nm spectral width, a pulse duration of 60 fs, and pulse to pulse energy fluctuations

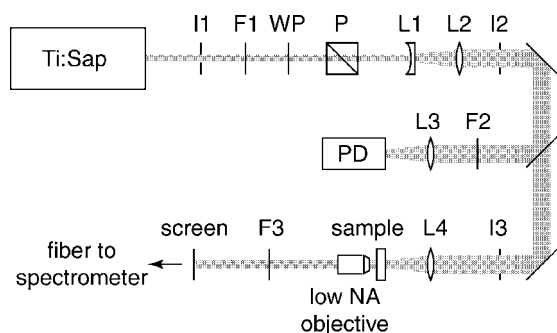


Fig. 1. Schematic of the setup used for damage and supercontinuum experiments. I1, I2, I3, iris; F1, F2, F3, neutral density filter wheels; WP, waveplate; P, polarizer; L1, L2, 3 $\times$  telescope; L3, 0.2 m focal lens; L4, sample focusing lens-objective (varied throughout experiment); PD, photodiode. All collection optics are UV-grade fused silica transparent down to 300 nm.

below 2%. Amplification is required to reach the critical power for self-focusing (about 300 nJ for a 60 fs pulse<sup>7,15</sup>). Additionally, the low repetition rate of the laser allows the sample to be translated during irradiation so that each successive pulse hits an unexposed area.

All experiments were carried out on UV-grade fused silica samples (ESCO commercial quality SI-UV; <5 waves/inch; 60-40 scratch-dig or better surface quality). For the experiments carried out at focusing conditions below 0.1 NA, we used 12 mm thick samples to ensure that all high-intensity propagation was confined to the bulk. At higher NAs we used thinner (1.0 and 3.0 mm) samples.

A schematic of the experimental setup is shown in Fig. 1. Because the key parameter in this study is the focusing angle of the incident pulse, beam quality is of critical importance. We therefore spatially filtered the 6 mm unfocused beam exiting the laser system using an iris (I1) so that a small section (approximately 0.5 mm in diameter) of the beam of relatively uniform intensity passes through, diffracting into an Airy pattern in the far field. This mode propagates 3 m and is then expanded by a factor of 3 using a telescope (L1, L2). A second iris (I2) spatially filters the central spot of the Airy pattern. This central spot, which is nearly Gaussian, is imaged with a CCD camera to measure mode shape and spot size. A fraction of the transmitted beam, which has a  $1/e^2$  diameter of about 7–8 mm, is split off and focused onto a calibrated photodiode (PD) to monitor the energy of each pulse incident on the sample. The pulse energy can be varied continuously over a large range using a combination of a half-waveplate (WP) and a Glan-laser polarizer (P), as well as a filter wheel (F1) that spans 3 OD (optical density) in 0.1 OD steps.

To focus at low NAs we used commercial BK7 and fused silica singlet lenses with focal lengths ranging from 300 mm to 50 mm. Using these lenses and a beam diameter of 7–8 mm we obtained NAs between 0.01 and 0.08. Above 0.16 NA, the spherical aberration introduced by a singlet lens degrades diffraction-limited focusing, so we used microscope objectives to obtain diffraction-limited spots at NAs ranging from 0.10 to 0.65. We observe that the damage threshold plateaus or has a slight minimum with the focus at a depth of roughly two confocal param-

eters. Therefore, we choose two confocal parameters as the depth for consistent bulk damage threshold measurements.

The BK7 and fused silica singlet lenses do not introduce appreciable dispersion [approximately  $-160 \text{ ps km}^{-1} \text{ nm}^{-1}$  (Ref. 16)], and therefore the pulse duration was minimized at the input of the focusing lens. The multiple elements and different glasses in high-NA microscope objectives, however, cause significant dispersion, and so the pulse must be prechirped to compensate for this dispersion. We therefore adjusted the grating pulse compressor to obtain the lowest energy damage threshold in the sample. The pulse width at the focus is then roughly equal to the shortest pulse duration measured in front of the objective.<sup>17</sup>

### A. Experimental Procedure—Supercontinuum Generation

As the threshold for supercontinuum generation we use the energy required to broaden the pulse spectrum such that 720 nm radiation is just visible to the dark-adapted eye. The supercontinuum generated is passed through a Schott BG40 filter, which passes the visible and begins to cut on strongly around 600 nm, to block the intense 800 nm portion of the spectrum. We chose this criterion because 720 nm is near the long-wavelength edge of the asymmetric blue-broadening characteristic of supercontinuum generation. Once we determined the energy threshold for a given NA, we increased the pulse energy by 60% and 100% and recorded the resulting supercontinuum spectra. Because at some NAs damage occurs below the supercontinuum threshold, the sample is continuously translated at 20 mm/s while spectra are collected, so that each pulse is incident on a fresh section of the sample.

Figure 2 shows a typical supercontinuum spectrum. An important metric for evaluating the supercontinuum is the extent to which the spectrum has been blue broadened. The edge of the blue broadening is chosen as the

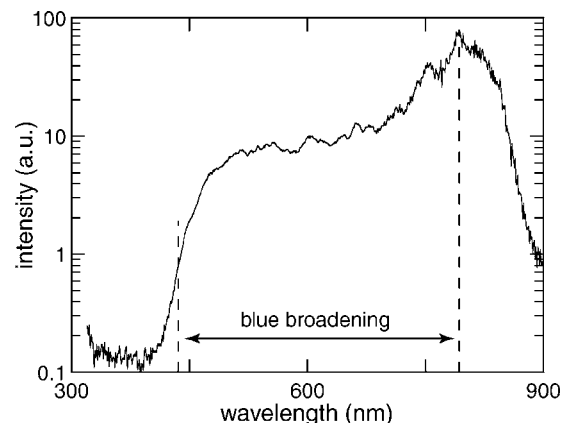


Fig. 2. Typical supercontinuum spectrum produced by a 60 fs, 480 nJ 800 nm laser pulse (1.6 times the supercontinuum threshold) focused at 0.025 NA. The value at the 800 nm peak is attenuated due to the spectrometer's limited dynamic range (typically, the pedestal is down by 100 to 500 times). The blue-broadening width is measured from the laser's center wavelength (800 nm) to the wavelength where the intensity of the supercontinuum spectrum is reduced to 10% of its plateau value.

wavelength where the intensity has dropped to 10% of the average intensity of the flat pedestal (dashed line in Fig. 2). The blue broadening is defined as the difference in photon energy between this edge and the 800 nm seed pulse, as indicated in Fig. 2.

### B. Experimental Procedure—Bulk Damage

We measured the damage threshold using a previously reported scattering technique.<sup>18</sup> A He–Ne probe laser beam propagates collinearly with the femtosecond laser pulse and reaches a focus at the same spot as the femtosecond laser. A beam block prevents the undisturbed He–Ne signal from reaching the detector. The damage threshold is determined by capturing the scattering of a He–Ne laser probe beam caused by material modification at the focal spot and recording it on a PD.

Contrary to the damage produced by longer pulses, femtosecond pulse-induced damage exhibits a sharp intensity threshold.<sup>3,19,20</sup> We observe that the measured value of this threshold (using the pulse energy as a metric) depends on the incident number of shots because both the size of the damage structure and the magnitude of the index change increase with each successive laser shot, and the scattering technique has a lower limit of sensitivity. We investigated this dependence by measuring the He–Ne scattered signal versus pulse energy at a number of NAs, for 1 to 10,000 incident pulses. The energy damage threshold ( $E_{th}^D$ ) decreases with an increasing number of pulses and plateaus as the number of pulses per spot increases to 5000 pulses (confirmed for NAs of 0.1, 0.25, 0.45, and 0.65). This measurement calibrates the scattering apparatus, and hence the damage threshold we report is for 5000-pulses. For these damage threshold measurements, the sample is stationary for the duration of a given 5000-pulse exposure, and then translated to a fresh region prior to continuing the experiment.

## 3. RESULTS

Figure 3 shows how the extent of the blue broadening decreases with increasing NA. The data obtained at both 1.6 and 2.0 times the supercontinuum threshold energy ( $E_{th}^S$ ) show the same trend, emphasizing that weak focusing should be used to obtain the broadest supercontinuum spectrum. Around 0.05 NA the shape of the spectrum

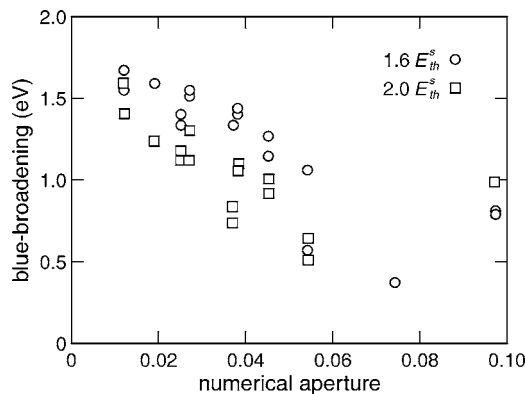


Fig. 3. NA dependence of the blue broadening at two different pulse energies.

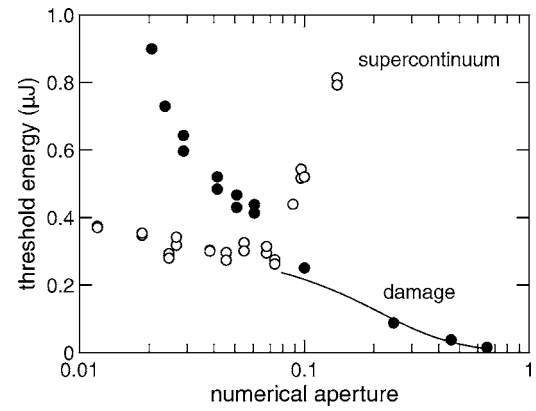


Fig. 4. Energy thresholds for damage (filled circles) and supercontinuum generation (open circles) versus NA. The black curve is a constant peak intensity fit of Eq. (1) to the damage data obtained for NAs above 0.1.

changes: at a lower NA the spectrum shows the characteristic blue-broadened pedestal seen in Fig. 2; at higher NAs the broadening is much more symmetric. Above 0.05 NA the supercontinuum generation also decreases when thousands of successive pulses are incident on the same spot, suggesting a slow buildup of damage. Above 0.1 NA, the damage threshold is lower than the supercontinuum generation threshold and plasma emission may contribute to the recorded spectrum<sup>21</sup> resulting in unreliable data for the blue broadening.

Figure 4 shows how the energy thresholds for supercontinuum generation and bulk damage depend on the NA. Below 0.07 NA, the threshold for supercontinuum generation is roughly constant at 300 nJ. Above 0.07 NA, however, the threshold quickly increases, and by 0.25 NA, no supercontinuum is observed up to the highest pulse energy, 10  $\mu$ J, available.

The threshold power for the onset of supercontinuum generation is the same as the critical power for self-focusing in a wide range of transparent materials,<sup>10,22–24</sup> supporting the hypothesis that supercontinuum generation is triggered by self-focusing. For the 60 fs pulse used in this experiment, the threshold energy value for supercontinuum generation of 300 nJ corresponds to a peak power of 4.9 MW, roughly consistent with the 4.3 MW critical power for self-focusing in fused silica.<sup>8,18</sup>

For pulse energies below the energy corresponding to the critical power, the effects of self-focusing can be taken into account and the focused spot size can be reliably predicted,<sup>25</sup> yielding the following relation between pulse energy, intensity, and NA:

$$E = \frac{I\tau\lambda^2}{0.9} \left[ 2\pi \frac{NA^2}{1 - NA^2} + \frac{I\lambda^2}{P_{crit}} \right]^{-1}. \quad (1)$$

Using the critical power  $P_{crit} = 4.9$  MW obtained above, we can fit this expression to the three damage threshold data points with  $NA > 0.10$  using the intensity as a fitting parameter. The result is shown in Fig. 4, and yields a threshold of  $1.0 \times 10^{18}$  W/m<sup>2</sup> (67 kJ/m<sup>2</sup> peak fluence), consistent with the breakdown intensities reported for other transparent materials of similar bandgap.<sup>2,18,19,26–28</sup> The fit becomes inaccurate as the threshold energy approaches the energy associated with the critical power

and the assumption of weak self-focusing is no longer valid.

Figure 5 shows the scattering of He–Ne laser light due to bulk damage as a function of incident pulse energy for three different NAs. As can be seen for 0.45 NA, there is a sharp energy damage threshold, indicated by the abrupt linear increase in the scattered signal. We do not observe such a sharp threshold at NAs below 0.1; instead the scattering intensity gradually increases as the pulse energy is increased (see, e.g., the data for 0.035 NA in Fig. 5). The sharp threshold exhibited in the high NA regime (0.25 NA or greater) is generally associated with the onset of multiphoton ionization.<sup>3,18–20,27,29</sup> Our data therefore suggest that the damage observed at NAs above 0.1 are due to multiphoton ionization of the material at the focus. The gradual increase in scattering observed below 0.1 NA suggests that a different mechanism is at play at these lower NAs.

Previous work has shown that at a high NA (0.65 to 1.4 NA) and pulse energies near the damage threshold, the extent of the damage is found to be roughly equal in size to the focal volume.<sup>30</sup> At energies significantly above threshold, the threshold intensity for damage is reached

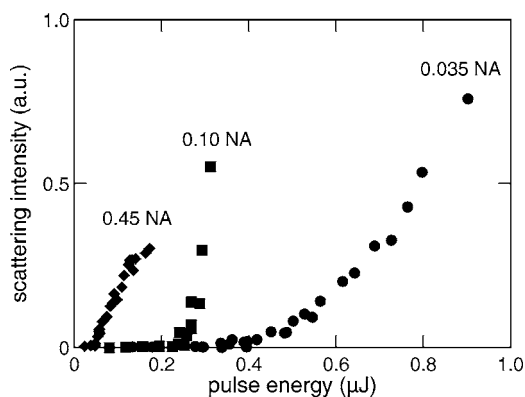


Fig. 5. Dependence of the He–Ne laser scattering signal on pulse energy and NA. For each data point the scattering intensity was determined after accumulating 5000 pulses on a single spot in the sample.

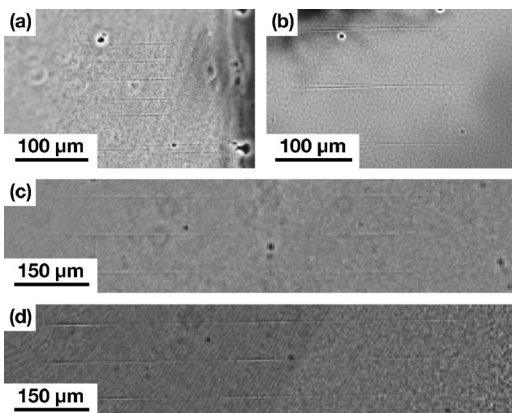


Fig. 6. Contrast-enhanced microscopy images of bulk damage in fused silica at low NA. The laser pulse is incident from the right. Vertically offset lines represent multiple repetitions of the experiment. The images are for an exposure of 10,000 pulses with (a) 0.055 NA at two times the damage threshold ( $2E_{th}^D$ ), (b) 0.033 NA at  $3E_{th}^D$ , (c) 0.019 NA at  $2E_{th}^D$ , and (d) 0.020 NA at  $3E_{th}^D$ .

early in the pulse, as the leading edge reaches the focus. However, the more intense regions of the pulse produce above-threshold intensities in front of the focus, where the spot size is larger, resulting in a cone-shaped damage area.<sup>30</sup> We used side-view optical microscopy to confirm that damage was confined to the bulk and to determine if there is any change in the damage morphology as the NA is lowered. To this end we polished two opposite thin sides of a 1.5 mm thick, 25 mm  $\times$  25 mm square sample of fused silica and exposed the sample with the polished edges normal to the incident beam at NAs ranging from 0.019 to 0.25 and energies from threshold to nearly ten times threshold. Because the damage generated at a low shot number does not yield significant changes in the index of refraction, each spot was exposed to 10,000 pulses. In all cases, the damage is confined to the bulk; we did not observe any surface damage.

As in the previous study, our results showed that in the high NA regime the structures produced in the bulk near the energy threshold match the confocal parameter in length, but for low NAs the structures are shorter than the confocal parameter. Figure 6 shows representative optical microscope images of the 10,000-pulse damage in the medium and low NA regime. At 0.055 NA the confocal parameter is 255  $\mu$ m, but the structures produced near the threshold energy extend for only 130  $\mu$ m [Fig. 6(a)]. As the NA is reduced, the discrepancy between the confocal parameter and the length of the structure increases. At 0.033 NA the structures begin to include the conical region in front of the focus [Fig. 6(b)]. Including this conical region the observable structure is only about 230  $\mu$ m long, while the confocal parameter is about 700  $\mu$ m. At 0.023 NA, the confocal parameter is 1.4 mm, but the structure length near the threshold is only 290  $\mu$ m long. At 0.019 NA the damage structures break up into two disconnected regions [see Fig. 6(c)], but the overall length of the structures is still much shorter than the confocal parameter.

In the low NA regime, the damage structures break up as the energy is increased to several times the energy threshold. For example, at 0.033 NA the single, cone-shaped damage structure seen in Fig. 6(b) breaks up into two regions similar to those seen in Fig. 6(c) when the energy is increased to four times the energy threshold. The region closest to the source is still cone shaped; the second region is located farther away from the source and is line shaped. The breaking up of the damage structures thus depends not only on the focusing conditions, but also on the laser energy.

We also investigated the dependence of the damage morphology on the number of laser pulses. To this end we made a series of damage structures at 0.020 NA and three times the energy threshold varying the number of laser pulses. At 1000 pulses two zones of damage are visible and at 5000 pulses a third zone becomes visible downstream. As more pulses accumulate, the three zones become more clearly visible [see Fig. 6(d)].

## 4. DISCUSSION

Our results indicate that the interaction of femtosecond laser pulses with transparent materials falls into three

regimes, depending on NA. For NAs larger than 0.25, we observe bulk damage above a certain pulse energy threshold but never any supercontinuum. In the range from 0.15 to 0.05 NA, we observe supercontinuum generation but multiple shots show the accumulation of bulk damage, causing the supercontinuum to disappear over time. Finally, below 0.05 NA, it is possible to damage the bulk, but only at energies significantly above the threshold for supercontinuum generation.

In the high-NA regime, the laser pulse energy at the damage threshold is not high enough to reach the critical power for self-focusing, and hence the external focusing dominates. The beam converges rapidly, producing intensities around  $10^{18}$  W/m<sup>2</sup> and creating a carrier density of approximately  $10^{27}$  m<sup>-3</sup> via nonlinear absorption.<sup>3</sup> Most of the pulse energy is thus deposited into the material at the focal volume either through nonlinear absorption or subsequent linear absorption by the plasma, resulting in bulk damage. What is left of the pulse quickly diverges after the focus. Because the pulse does not propagate at high intensity for an appreciable distance there is no interaction length over which self-phase modulation can accumulate or an optical shock can form and so no supercontinuum is generated.<sup>14</sup> Even at pulse energies exceeding the critical power we observe no supercontinuum. The absorption of energy at the focus prevents the subsequent recollapse of the pulse via self-focusing. Indeed, a previous study<sup>18</sup> confirmed that when  $3 \mu\text{J}$ , 110 fs pulses are focused into fused silica at 0.65 NA, the energy remaining in the pulse after propagation through the focus is always below the critical power at that pulse width.

At low NA, self-focusing increases the pulse intensity as it propagates through the sample. The increasing intensity creates a low-density electron plasma ( $10^{24}$  m<sup>-3</sup>) that counteracts self-focusing,<sup>8,14,15</sup> prevents the formation of a critical density plasma, and prevents single-shot damage at energies available in our experiments. Supercontinuum is generated by the accumulation of self-phase modulation, self-steepening, and space-time focusing while the pulse propagates as a filament.<sup>14,31,32</sup> As the NA is increased, the confocal parameter becomes smaller, yielding a shorter interaction length and therefore less blue-broadening.

The NA regime simply represents the transition between these two extremes. As the NA is decreased and the focused spot size increases, more energy is required to reach the breakdown intensity, bringing the pulse closer to or above the critical power for self-focusing. The more that self-focusing dominates the effects of the external focusing (NA), the closer the interaction moves toward the low-NA regime.

The optical microscopy images in Fig. 6 and the scattering intensity data suggest that the damage mechanism is different in the low- and high-NA regimes. The low-NA damage shows filaments that are much shorter than the confocal parameter of the external focusing. Also, there is no sharp energy threshold for damage at low NA (Fig. 5). It is possible that the supercontinuum that occurs at low NA causes color center formation or densification. Indeed, the formation of color centers was observed in the bulk of some silicate glasses under weakly focused femtosecond

irradiation.<sup>33</sup> This color center formation was attributed to the linear and two-photon absorption of the blue edge of the supercontinuum.<sup>33</sup> Additionally, ultraviolet radiation is known to cause densification of silica<sup>34</sup> and is widely used in the writing of fiber Bragg gratings.<sup>35</sup> At a high NA, on the other hand, the damage mechanism can be attributed to a combination of multiphoton absorption and avalanche ionization.<sup>3,18–20,27,29</sup>

The breaking up of the damage structures shown in Figs. 6(c) and 6(d) can be attributed to the refocusing of femtosecond pulses in fused silica. Refocusing of femtosecond beams has been modeled<sup>36,37</sup> and observed in air<sup>38</sup> and liquids<sup>39</sup> and imaged by plasma emission in solids at high<sup>40</sup> and low<sup>41</sup> NAs. The multiple zones of damage we observe at a low NA are consistent with the observed plasma emission due to refocusing of femtosecond laser beams in fused silica.<sup>41</sup>

In conclusion, we studied the role of the NA of the external focusing in the interaction of femtosecond laser pulses with transparent materials. At a high NA (above 0.25 NA), single-shot, catastrophic damage occurs, and no supercontinuum generation is observed. Below 0.15 NA we observe supercontinuum generation and damage at a threshold significantly above the threshold for supercontinuum generation. Bulk micromachining is only practical for NAs of 0.25 NA and above, where self-focusing effects are minimal and spot size and focal position can be accurately predicted and controlled. Further, as the NA is increased, the energy necessary to cause material modification decreases, minimizing collateral damage. While supercontinuum can be produced at any NA below 0.15 NA, the spectrum is broadest at the lowest NA. Also, at the lowest NA, the supercontinuum is produced well below the damage threshold. Below 0.05 NA we observe multiple refocusing of the femtosecond laser beam. The results presented in this paper show that the NA, a linear optical parameter which is independent of the laser parameters, controls the interaction of ultrashort laser pulses with transparent materials, a highly nonlinear process.

## ACKNOWLEDGMENTS

The research described in this paper was supported by the National Science Foundation under contracts PHY-998123 and DMI-0334984, and the Army Research Office under contract W911NF-05-1-0471. The authors would also like to acknowledge the use of the facilities of the Center for Nanoscale Systems, which is supported by the National Science Foundation's National Nanotechnology Infrastructure Network.

\*Present address, MIT Lincoln Laboratory, Lexington, MA 02420.

†Present address, Department of Biomedical Engineering, Cornell University, Ithaca, NY 14853.

## REFERENCES

1. E. N. Glezer, M. Milosavljevic, L. Huang, R. J. Finlay, T. H. Her, J. P. Callan, and E. Mazur, "Three-dimensional optical storage inside transparent materials," *Opt. Lett.* **21**, 2023–2025 (1996).

2. A. C. Tien, S. Backus, H. Kapteyn, M. Murnane, and G. Mourou, "Short-pulse laser damage in transparent materials as a function of pulse duration," *Phys. Rev. Lett.* **82**, 3883–3886 (1999).
3. B. C. Stuart, M. D. Feit, S. Herman, A. M. Rubenchik, B. W. Shore, and M. D. Perry, "Nanosecond-to-femtosecond laser-induced breakdown in dielectrics," *Phys. Rev. B* **53**, 1749–1761 (1996).
4. D. Ashkenasi, H. Varel, A. Rosenfeld, S. Henz, J. Herrmann, and E. E. B. Cambell, "Application of self-focusing of ps laser pulses for three-dimensional microstructuring of transparent materials," *Appl. Phys. Lett.* **72**, 1442–1444 (1998).
5. K. Yamada, W. Watanabe, T. Toma, K. Itoh, and J. Nishii, "*In situ* observation of photoinduced refractive-index changes in filaments formed in glasses by femtosecond laser pulses," *Opt. Lett.* **26**, 19–21 (2001).
6. R. R. Alfano and S. L. Shapiro, "Observation of self-phase modulation and small-scale filaments in crystals and glasses," *Phys. Rev. Lett.* **24**, 592–594 (1970).
7. A. Brodeur and S. L. Chin, "Ultrafast white-light continuum generation and self-focusing in transparent condensed media," *J. Opt. Soc. Am. B* **16**, 637–650 (1999).
8. A. Brodeur and S. L. Chin, "Band-gap dependence of the ultrafast white-light continuum," *Phys. Rev. Lett.* **80**, 4406–4409 (1998).
9. N. T. Nguyen, A. Salimnia, W. Liu, S. L. Chin, and R. Vallee, "Optical breakdown versus filamentation in fused silica by use of femtosecond infrared laser pulses," *Opt. Lett.* **28**, 1591–1593 (2003).
10. F. A. Ilkov, L. S. Ilkova, and S. L. Chin, "Supercontinuum generation versus optical-breakdown in CO<sub>2</sub> gas," *Opt. Lett.* **18**, 681–683 (1993).
11. Q. Feng, J. V. Moloney, A. C. Newell, and E. M. Wright, "Laser-induced breakdown versus self-focusing for focused picosecond pulses in water," *Opt. Lett.* **20**, 1958–1960 (1995).
12. W. Liu, O. Kosareva, I. S. Golubtsov, A. Iwasaki, A. Becker, V. P. Kandidov, and S. L. Chin, "Femtosecond laser pulse filamentation versus optical breakdown in H<sub>2</sub>O," *Appl. Phys. B* **76**, 215–229 (2003).
13. M. R. Junnarkar, "Short pulse propagation in tight focusing conditions," *Opt. Commun.* **195**, 273–292 (2001).
14. A. L. Gaeta, "Catastrophic collapse of ultrashort pulses," *Phys. Rev. Lett.* **84**, 3582–3585 (2000).
15. J. H. Marburger, "Self-focusing: theory," *Prog. Quantum Electron.* **4**, 35–110 (1975).
16. B. E. A. Saleh and M. C. Teich, *Fundamentals of Photonics*, Wiley Series in Pure and Applied Optics (Wiley, 1991), pp. xviii.
17. M. Muller, J. Squier, and G. J. Brakenhoff, "Measurement of femtosecond pulses in the focal point of a high-numerical-aperture lens by two-photon absorption," *Opt. Lett.* **20**, 1038–1040 (1995).
18. C. B. Schaffer, A. Brodeur, and E. Mazur, "Laser-induced breakdown and damage in bulk transparent materials induced by tightly focused femtosecond laser pulses," *Meas. Sci. Technol.* **12**, 1784–1794 (2001).
19. B. C. Stuart, M. D. Feit, S. Herman, A. M. Rubenchik, B. W. Shore, and M. D. Perry, "Optical ablation by high-power short-pulse lasers," *J. Opt. Soc. Am. B* **13**, 459–468 (1996).
20. D. Du, X. Liu, G. Korn, J. Squier, and G. Mourou, "Laser-induced breakdown by impact ionization in SiO<sub>2</sub> with pulse widths from 7 ns to 150 fs," *Appl. Phys. Lett.* **64**, 3071–3073 (1994).
21. C. W. Carr, M. D. Feit, A. M. Rubenchik, P. De Mange, S. O. Kucheyev, M. D. Shirk, H. B. Radousky, and S. G. Demos, "Radiation produced by femtosecond laser-plasma interaction during dielectric breakdown," *Opt. Lett.* **30**, 661–663 (2005).
22. W. L. Smith, P. Liu, and N. Bloembergen, "Superbroadening in H<sub>2</sub>O and D<sub>2</sub>O by self-focused picosecond pulses from a YAlG:Nd laser," *Phys. Rev. A* **15**, 2396–2403 (1977).
23. P. B. Corkum, C. Rolland, and T. Srinivasanrao, "Supercontinuum generation in gases," *Phys. Rev. Lett.* **57**, 2268–2271 (1986).
24. J. K. Ranka, R. W. Schirmer, and A. L. Gaeta, "Observation of pulse splitting in nonlinear dispersive media," *Phys. Rev. Lett.* **77**, 3783–3786 (1996).
25. S. A. Akhmanov, R. V. Khokhlov, and A. P. Sukhorukov, "Self-focusing, self-defocusing and self-modulation of laser beams," in *Laser Handbook*, F. T. Arecchi, E. O. Schulz-Dubois, and M. L. Stitch, eds. (North-Holland, American Elsevier, 1972).
26. D. Du, X. Liu, and G. Mourou, "Reduction of multi-photon ionization in dielectrics due to collisions," *Appl. Phys. B* **63**, 617–621 (1996).
27. M. Lenzner, J. Kruger, S. Sartania, Z. Cheng, C. Spielmann, G. Mourou, W. Kautek, and F. Krausz, "Femtosecond optical breakdown in dielectrics," *Phys. Rev. Lett.* **80**, 4076–4079 (1998).
28. D. von der Linde and H. Schuler, "Breakdown threshold and plasma formation in femtosecond laser-solid interaction," *J. Opt. Soc. Am. B* **13**, 216–222 (1996).
29. W. Kautek, J. Kruger, M. Lenzner, S. Sartania, C. Spielmann, and F. Krausz, "Laser ablation of dielectrics with pulse durations between 20 fs and 3 ps," *Appl. Phys. Lett.* **69**, 3146–3148 (1996).
30. C. B. Schaffer, A. O. Jamison, and E. Mazur, "Morphology of femtosecond laser-induced structural changes in bulk transparent materials," *Appl. Phys. Lett.* **84**, 1441–1443 (2004).
31. F. Demartini, C. H. Townes, T. K. Gustafso, and P. L. Kelley, "Self-steepening of light pulses," *Phys. Rev.* **164**, 312–323 (1967).
32. J. E. Rothenberg, "Space-time focusing: breakdown of the slowly varying envelope approximation in the self-focusing of femtosecond pulses," *Opt. Lett.* **17**, 1340–1342 (1992).
33. O. M. Efimov, K. Gabel, S. V. Garnov, L. B. Glebov, S. Grantham, M. Richardson, and M. J. Soileau, "Color-center generation in silicate glasses exposed to infrared femtosecond pulses," *J. Opt. Soc. Am. B* **15**, 193–199 (1998).
34. D. C. Allan, C. Smith, N. F. Borrelli, and T. P. Seward, "193-nm excimer-laser-induced densification of fused silica," *Opt. Lett.* **21**, 1960–1962 (1996).
35. K. O. Hill, Y. Fujii, D. C. Johnson, and B. S. Kawasaki, "Photosensitivity in optical fiber waveguides—application to reflection filter fabrication," *Appl. Phys. Lett.* **32**, 647–649 (1978).
36. M. Mlejnek, M. Kolesik, E. M. Wright, and J. V. Moloney, "Recurrent femtosecond pulse collapse in air due to plasma generation: numerical results," *Math. Comput. Simul.* **56**, 563–570 (2001).
37. M. Mlejnek, E. M. Wright, and J. V. Moloney, "Dynamic spatial replenishment of femtosecond pulses propagating in air," *Opt. Lett.* **23**, 382–384 (1998).
38. A. Talebpour, S. Petit, and S. L. Chin, "Re-focusing during the propagation of a focused femtosecond Ti:sapphire laser pulse in air," *Opt. Commun.* **171**, 285–290 (1999).
39. W. Liu, S. L. Chin, O. Kosareva, I. S. Golubtsov, and V. P. Kandidov, "Multiple refocusing of a femtosecond laser pulse in a dispersive liquid (methanol)," *Opt. Commun.* **225**, 193–209 (2003).
40. Z. X. Wu, H. B. Jiang, L. Luo, H. C. Guo, H. Yang, and Q. H. Gong, "Multiple foci and a long filament observed with focused femtosecond pulse propagation in fused silica," *Opt. Lett.* **27**, 448–450 (2002).
41. Z. X. Wu, H. B. Jiang, H. Yang, and Q. H. Gong, "The refocusing behaviour of a focused femtosecond laser pulse in fused silica," *J. Opt. A, Pure Appl. Opt.* **5**, 102–107 (2003).